Обзор ArXiv: astro-ph, 11-15 сентября 2017

От Сильченко О.К.

Astro-ph: 1709.03542

The last 6 Gyr of dark matter assembly in massive galaxies from the Kilo Degree Survey

C. Tortora[1⋆], N.R. Napolitano[2], N. Roy[2,3], M. Radovich[4], F. Getman[2], L.V.E. Koopmans[1], G. A. Verdoes Kleijn[1], K. H. Kuijken[5]

[1] *Kapteyn Astronomical Institute, University of Groningen, P.O. Box 800, 9700 AV Groningen, the Netherlands*
[2] *INAF – Osservatorio Astronomico di Capodimonte, Salita Moiariello, 16, 80131 - Napoli, Italy*
[3] *Dipartimento di Scienze Fisiche, Università di Napoli Federico II, Compl. Univ. Monte S. Angelo, 80126 - Napoli, Italy*
[4] *INAF – Osservatorio Astronomico di Padova, Vicolo Osservatorio 5, 35122 - Padova, Italy*
[5] *Leiden Observatory, Leiden University, P.O. Box 9513, 2300 RA Leiden, the Netherlands*

Accepted Received

ABSTRACT

We study the dark matter (DM) assembly in the central regions of massive early-type galaxies up to $z \sim 0.65$. We use a sample of ~ 3800 massive ($\log M_\star/M_\odot > 11.2$) galaxies with photometry and structural parameters from 156 sq. deg. of the Kilo Degree Survey, and spectroscopic redshifts and velocity dispersions from SDSS. We obtain central total-to-stellar mass ratios, $M_{\rm dyn}/M_\star$, and DM fractions, by determining dynamical masses, $M_{\rm dyn}$, from Jeans modelling of SDSS aperture velocity dispersions and stellar masses, $M_\star$, from KiDS galaxy colours. We first show how the central DM

Выборка

SDSS area, starts to be incomplete at redshift $z \gtrsim 0.6$ and masses $\log M_*/M_\odot \gtrsim 11.3$. The fiber diameter is of 2 arcsec. Velocity dispersions are determined in Thomas et al. (2013), using Penalized PiXel Fitting (pPXF, Cappellari & Emsellem 2004) and GANDALF (Sarzi et al. 2006) on the BOSS spectra. These values are quite robust being, on average, quite similar to the measurements from independent literature (see Thomas et al. 2013 for further details).

The final sample consists of 4118 MPA-JHU-DR7 galaxies and 5603 BOSS-DR10 galaxies, for a total of 9721 systems with structural parameters, spectroscopic redshifts and velocity dispersions. We limit to a mass-completed sample of galaxies with $\log M_*/M_\odot > 11.2$, consisting of a total of 3778 galaxies with redshift $0 < z < 0.7$.

Шкалирующие соотношения

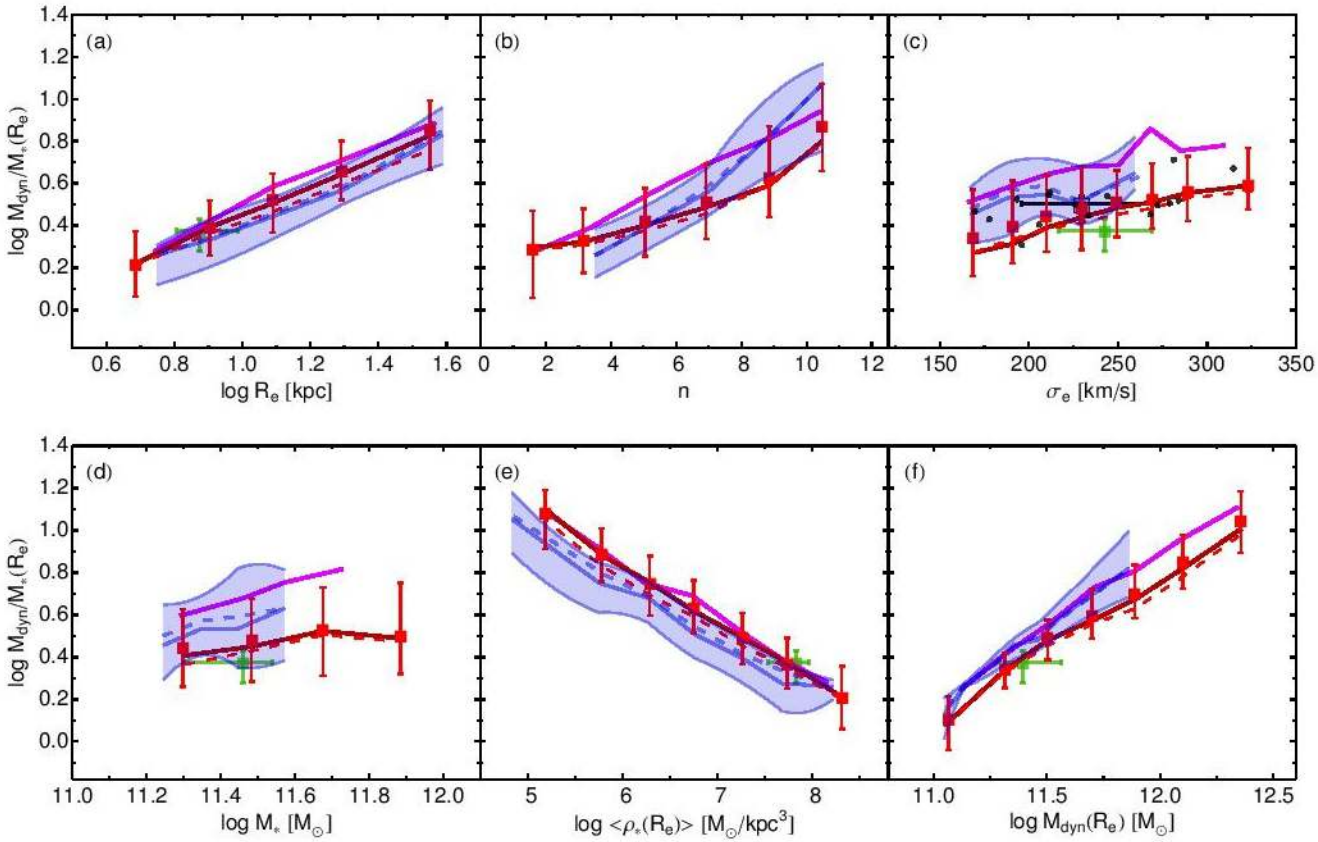

Зависимость от красного смещения

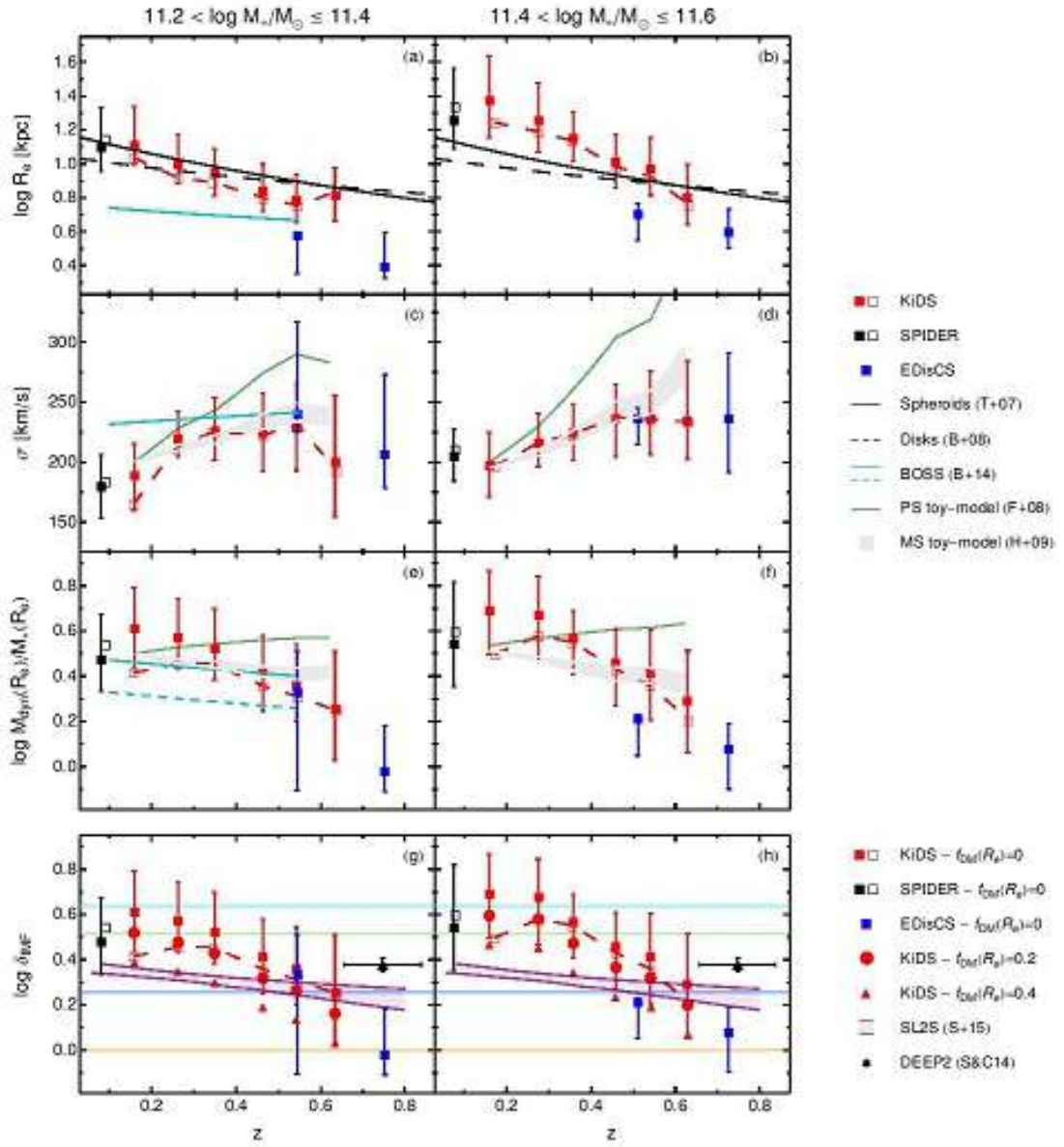

Работающая модель (справа)

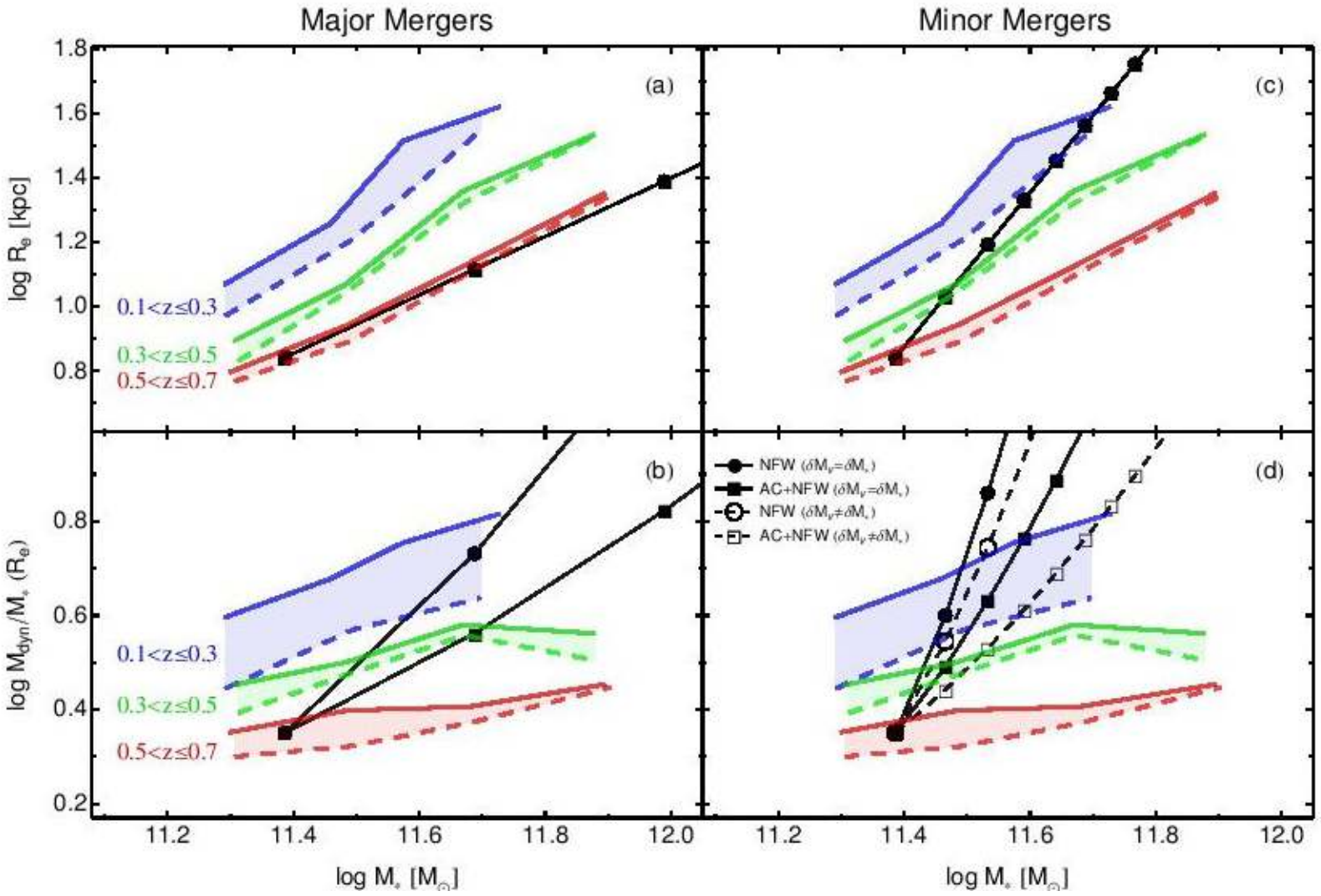

Astro-ph: 1709.03691

DETERMINING THE HALO MASS SCALE WHERE GALAXIES LOSE THEIR GAS.*

Gregory Rudnick[1,2], Pascale Jablonka[3,4], John Moustakas[5], Alfonso Aragón-Salamanca[6], Dennis Zaritsky[7], Yara L. Jaffé[8,9], Gabriella De Lucia[10], Vandana Desai[11], Claire Halliday[12], Dennis Just[7,13], Bo Milvang-Jensen[14], Bianca Poggianti[15]

Accepted for Publication in ApJ

ABSTRACT

A major question in galaxy formation is how the gas supply that fuels activity in galaxies is modulated by their environment. We use spectroscopy of a set of well characterized clusters and groups at $0.4 < z < 0.8$ from the ESO Distant Cluster Survey (EDisCS) and compare it to identically selected field galaxies. Our spectroscopy allows us to isolate galaxies that are dominated by old stellar populations. Here we study a stellar-mass limited sample ($\log(M_*/M_\odot) > 10.4$) of these old galaxies with weak [O II] emission. We use line ratios and compare to studies of local early type galaxies to conclude that this gas is likely excited by post-AGB stars and hence represents a diffuse gas component in the galaxies. For cluster and group galaxies the fraction with EW([O II])> 5Å is $f_{[OII]} = 0.08^{+0.03}_{-0.02}$ and $f_{[OII]} = 0.06^{+0.07}_{-0.04}$ respectively. For field galaxies we find $f_{[OII]} = 0.27^{+0.07}_{-0.06}$, representing a 2.8σ difference between the [O II] fractions for old galaxies between the different environments. We conclude that a population of old galaxies in all environments has ionized gas that likely stems from stellar mass loss. In the field galaxies also experience gas accretion from the cosmic web and in groups and clusters these galaxies have had their gas accretion shut off by their environment. Additionally, galaxies with emission preferentially avoid the virialized region of the cluster in position-velocity space. We discuss the implications of our results, among which is that gas accretion shutoff is likely effective at group halo masses ($\log \mathcal{M}/\mathcal{M}_\odot > 12.8$) and that there are likely multiple gas removal processes happening in dense environments.

Скопления и группы на z=0.6

Table 1
Cluster and Group Data

system	z	σ[a] [km/s]	N_{samp}[b]
		Clusters	
cl1018.8-1211	0.4734	486^{+59}_{-63}	17
cl1040.7-1155	0.7043	418^{+55}_{-46}	10
cl1054.4-1146	0.6972	589^{+78}_{-70}	26
cl1054.7-1245	0.7498	504^{+113}_{-65}	21
cl1059.2-1253	0.4564	510^{+52}_{-56}	26
cl1138.2-1133	0.4796	732^{+72}_{-76}	9
cl1138.2-1133a	0.4548	542^{+63}_{-71}	5
cl1202.7-1224	0.4240	518^{+92}_{-104}	9
cl1216.8-1201	0.7943	1018^{+73}_{-77}	42
cl1227.9-1138	0.6357	574^{+72}_{-75}	13
cl1232.5-1250	0.5414	1080^{+119}_{-89}	9
cl1301.7-1139	0.4828	687^{+81}_{-86}	18
cl1353.0-1137	0.5882	666^{+136}_{-139}	13
cl1354.2-1230	0.7620	648^{+105}_{-110}	11
cl1354.2-1230a	0.5952	433^{+95}_{-104}	6
cl1411.1-1148	0.5195	710^{+125}_{-133}	13

Table 1
Cluster and Group Data

system	z	σ[a] [km/s]	N_{samp}[b]
		Groups	
cl1037.9-1243	0.5783	319^{+53}_{-52}	7
cl1040.7-1155a	0.6316	179^{+40}_{-26}	6
cl1040.7-1155b	0.7798	259^{+91}_{-52}	2
cl1054.4-1146a	0.6130	227^{+72}_{-28}	5
cl1054.7-1245a	0.7305	182^{+58}_{-69}	9
cl1227.9-1138a	0.5826	341^{+42}_{-46}	1
cl1301.7-1139a	0.3969	391^{+63}_{-69}	10
cl1420.3-1236	0.4962	218^{+43}_{-50}	18

[a] This was computed using the full EDisCS member sample, which is larger than the sample used for the analysis in this paper.
[b] The number of galaxies meeting our stellar mass and quality cuts.

Параметры выборки

The EDisCS spectroscopic magnitude limit is $I = 22$ for $0.4 < z < 0.6$ clusters and $I = 23$ for $0.6 < z < 0.8$ clusters. The fainter selection at high redshift offsets the increasing luminosity distance and the same mass limit $\log(\mathcal{M}_\star/\mathcal{M}_\odot) > 10.4$, applies for all of our systems. In all of what follows we only consider galaxies above this limit. This results in a total of 163, 55, and 251 field, group and cluster galaxies respectively. In the last column of Table 1 we indicate the number of galaxies in this final sample that come from each cluster and group.

Разделение на молодые и старые звездные населения

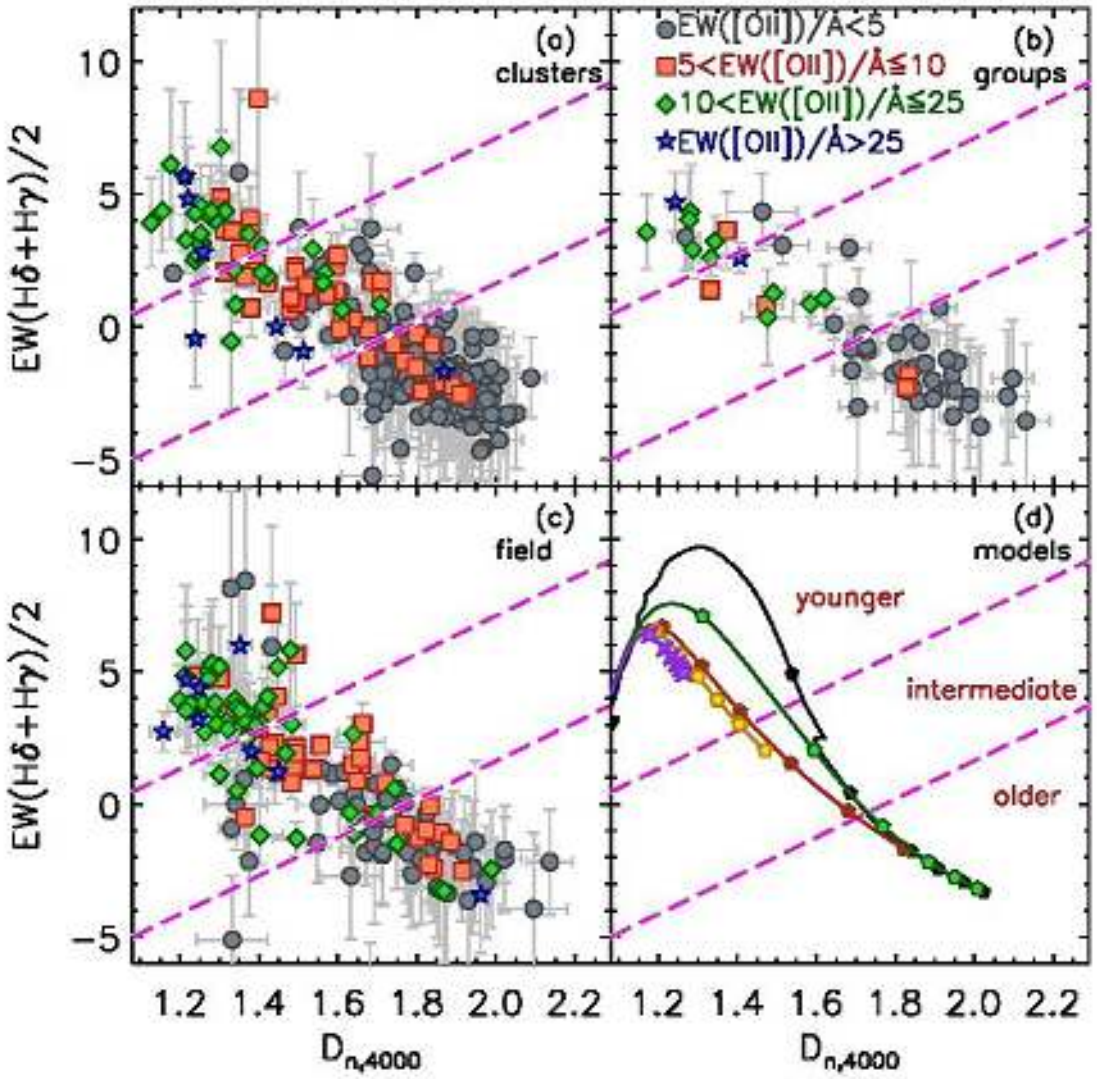

Характеристики выборки «молодых» и «старых» галактик в окружении разной плотности

Table 3
Fractions of emission-line galaxies as a function of stellar age and environment

Relative Age[a]	$f_{e,field}$[b]	$f_{e,group}$[b]	$f_{e,cluster}$[b]	$f_{e,group+cluster}$[b]	N_{field}	N_{group}	$N_{cluster}$
younger	$0.92^{+0.04}_{-0.06}$	$0.80^{+0.13}_{-0.21}$	$0.91^{+0.05}_{-0.08}$	$0.89^{+0.05}_{-0.07}$	50	10	35
intermediate	$0.60^{+0.07}_{-0.07}$	$0.58^{+0.17}_{-0.18}$	$0.56^{+0.07}_{-0.07}$	$0.56^{+0.06}_{-0.06}$	58	12	66
older	$0.27^{+0.07}_{-0.06}$	$0.06^{+0.08}_{-0.04}$	$0.08^{+0.03}_{-0.02}$	$0.08^{+0.02}_{-0.02}$	55	33	150

Note. — All errors on the fractions are computed using binomial errors. Galaxies are limited in stellar mass to $\log(\mathcal{M}_\star/\mathcal{M}_\odot) > 10.4$.. The numbers in the rightmost columns correspond to the total number of galaxies in each age-environment combination that pass all of our selection criteria.

[a] The relative ages corresponding to the age divisions in $D_n(4000)$-$\langle \mathrm{H}\delta_{abs}\mathrm{H}\gamma_{abs}\rangle$ plane as shown in Figure 1 and 2.

[b] The fraction of galaxies in each relative age bin and in each environment that have EW([O II])> 5Å.

Присутствие эмиссии [OII]3727

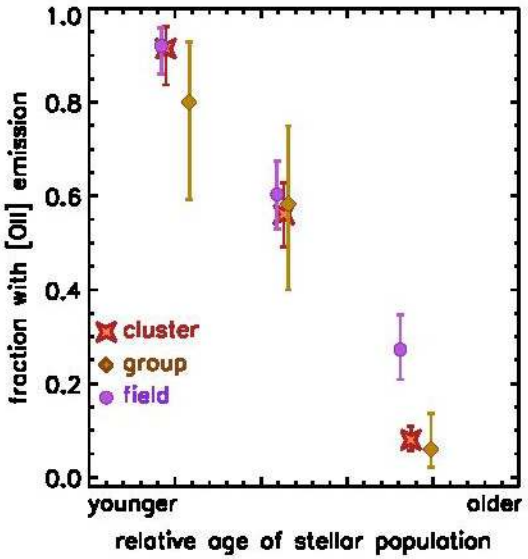

Figure 6. The fraction of galaxies with EW([O II])> 5Å as a function of relative stellar population age as defined in Fig. 1 and Fig. 2. The points have been shifted in the x-direction slightly with respect to one another so that they do not overlap. This plot demonstrates one of the key results of the paper, namely that old galaxies in the field have a higher fraction of [O II] emission than old galaxies in clusters and groups.

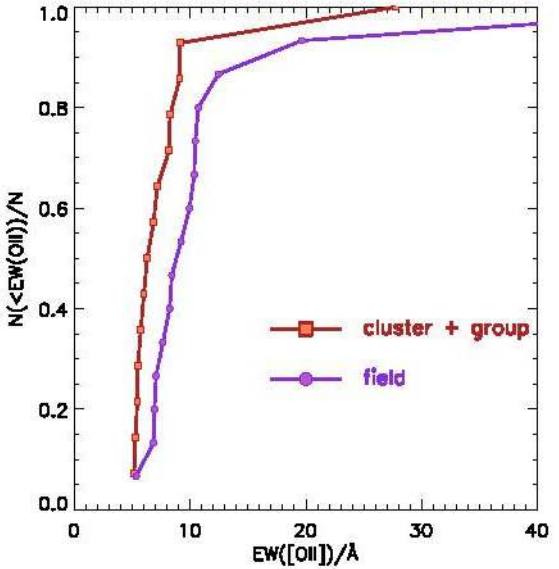

Figure 8. The cumulative distributions of EW([O II]) for galaxies with EW([O II])> 5Å that are classified as "older" based on $D_n(4000)$ and the $\langle H\delta_{abs} H\gamma_{abs}\rangle$ strength. The cluster+group distribution is shifted towards lower EW([O II]) values, with only a 3% K-S probability of being drawn from the same distribution as the field galaxies.

Динамика галактик в скоплениях

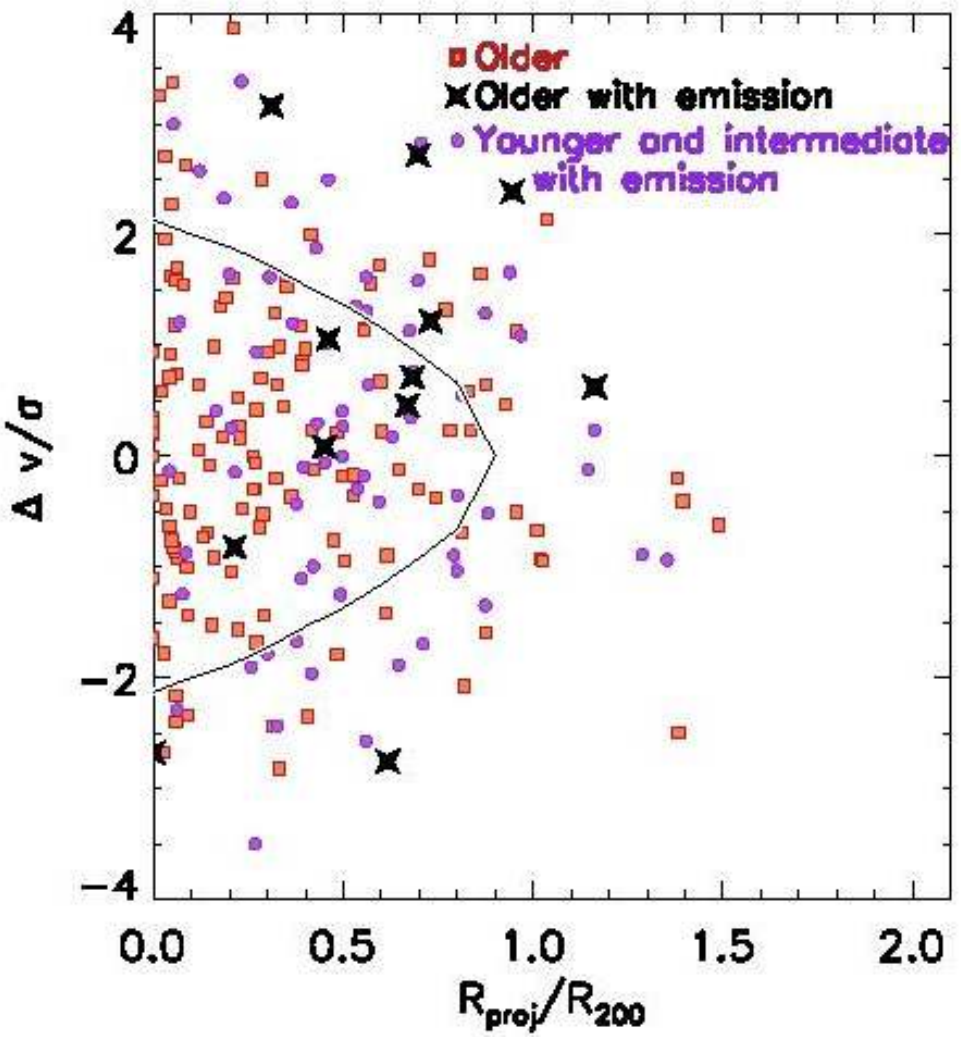

Всяческая статистика для «старых» галактик с эмиссиями

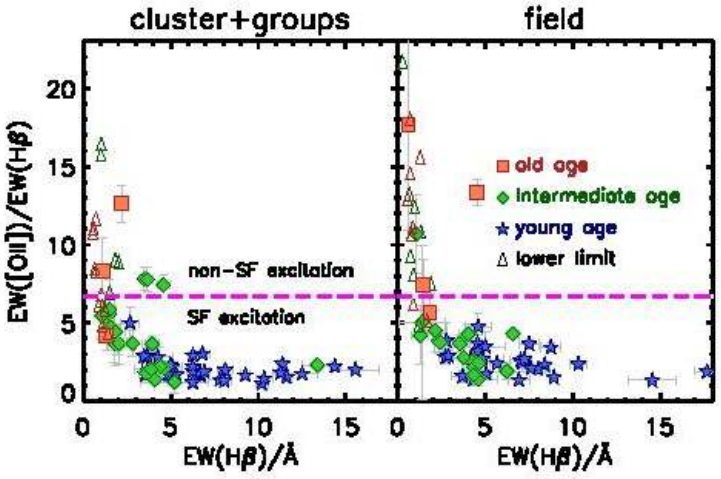

Figure 12. An AGN diagnostic diagram for all of the galaxies in our sample with EW([O II])> 5Å for which $H\beta$ could have been observed. All emission and absorption features have been decomposed as described in the text. Arrows are 1σ lower limits on the ratio, plotted at the 1σ upper limit of EW($H\beta_{em}$). Line ratios above the horizontal line cannot be powered by normal star formation (Sánchez-Blázquez et al. 2009).

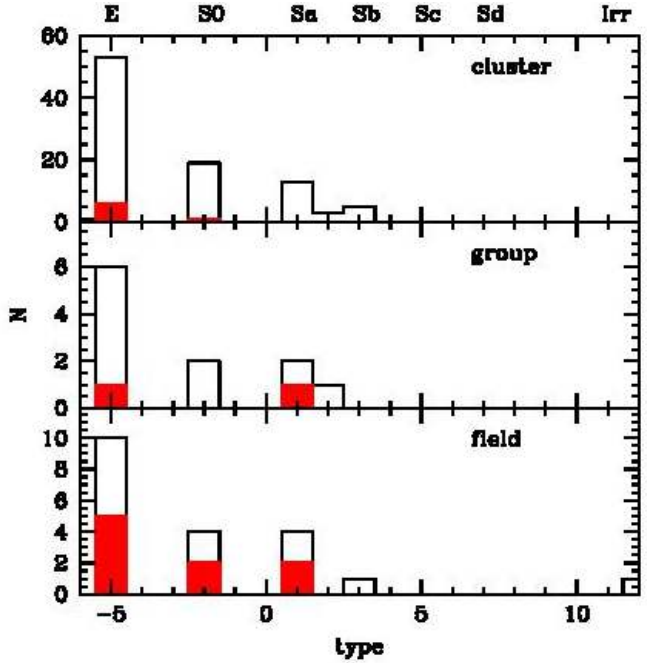

Figure 14. The distribution of morphological types for the "older" galaxies. The T-Type is given on the bottom axis and the Hubble Type on the top axis. The empty histogram is for all of these galaxies and the filled histogram is for the subset with EW([O II])> 5Å. The vertical scale is different in each panel. All but three of the "older" [O II] emitters have E/S0 morphology, indeed the early-type fraction of this subsample of galaxies is consistent at 1-σ across all environments. This indicates that the environmental difference in the EW([O II]) distribution of "older" galaxies cannot be driven by the morphology-density relation.

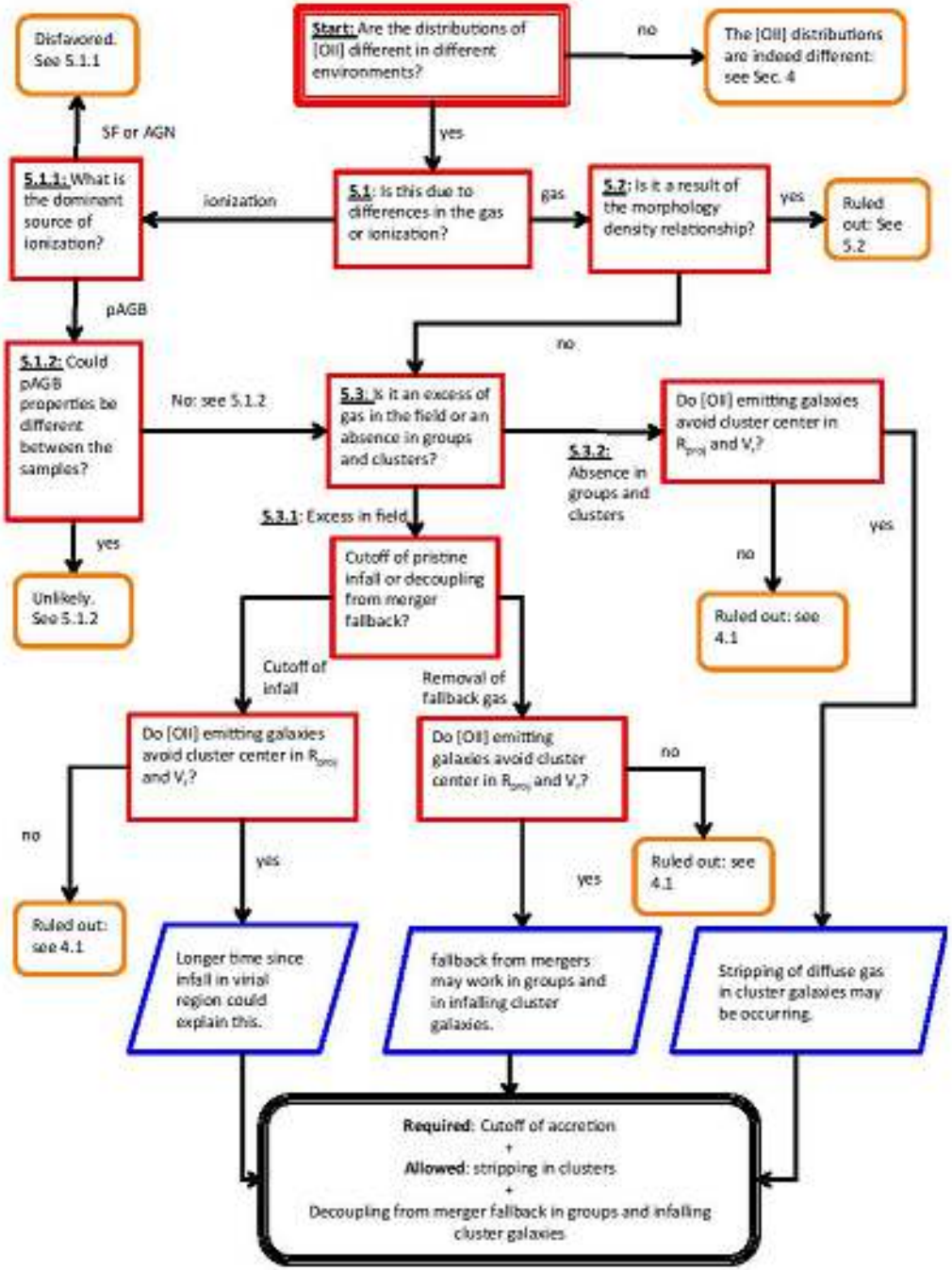
Start: Are the distributions of [OII] different in different environments?
no
The [OII] distributions are indeed different: see Sec. 4
yes
5.1: Is this due to differences in the gas or ionization?
ionization
gas
5.2: Is it a result of the morphology density relationship?
yes
Ruled out: See 5.2
5.1.1: What is the dominant source of ionization?
SF or AGN
Disfavored. See 5.1.1
pAGB
5.1.2: Could pAGB properties be different between the samples?
yes
Unlikely. See 5.1.2
No: see 5.1.2
5.3: Is it an excess of gas in the field or an absence in groups and clusters?
no
5.3.1: Excess in field
5.3.2: Absence in groups and clusters
Do [OII] emitting galaxies avoid cluster center in R_{proj} and V_r?
yes
no
Ruled out: see 4.1
Cutoff of pristine infall or decoupling from merger fallback?
Cutoff of infall
Removal of fallback gas
Do [OII] emitting galaxies avoid cluster center in R_{proj} and V_r?
no
yes
Ruled out: see 4.1
Do [OII] emitting galaxies avoid cluster center in R_{proj} and V_r?
no
yes
Ruled out: see 4.1
Longer time since infall in virial region could explain this.
fallback from mergers may work in groups and in infalling cluster galaxies.
Stripping of diffuse gas in cluster galaxies may be occurring.
Required: Cutoff of accretion
+
Allowed: stripping in clusters
+
Decoupling from merger fallback in groups and infalling cluster galaxies

Вывод из этой цепочки рассуждений:

- В поле идет аккреция внешнего газа на галактики ранних типов, а в скоплениях И В ГРУППАХ – нет, там газ только тот, что сброшен звездами.

Astro-ph: 1709.03988

A FUNDAMENTAL TEST FOR GALAXY FORMATION MODELS: MATCHING THE LYMAN-α ABSORPTION PROFILES OF GALACTIC HALOS OVER THREE DECADES IN DISTANCE

Daniele Sorini[1, 2] José Oñorbe[1], Joseph F. Hennawi[1, 3], Zarija Lukić[4]

Submitted to the AAS Journals

ABSTRACT

Galaxy formation depends critically on the physical state of gas in the circumgalactic medium (CGM) and its interface with the intergalactic medium (IGM), determined by the complex interplay between inflows from the IGM and outflows from supernovae and/or AGN feedback. The average Lyman-α absorption profile around galactic halos represents a powerful tool to probe their gaseous environments. We compare predictions from Illustris and Nyx hydrodynamical simulations with the observed absorption around foreground quasars, damped Lyman-α systems, and Lyman-break galaxies. We show how large-scale BOSS and small-scale quasar pair measurements can be combined to precisely constrain the absorption profile over three decades in transverse distance $20\,\mathrm{kpc} \lesssim b \lesssim 20\,\mathrm{Mpc}$. Far from galaxies $\gtrsim 2\,\mathrm{Mpc}$, the simulations converge to the same profile and provide a reasonable match to the observations. This asymptotic agreement arises because the ΛCDM model successfully describes the ambient IGM, and represents a critical advantage of studying the mean absorption profile. However, significant differences between the simulations, and between simulations and observations are present on scales $20\ \mathrm{kpc} \lesssim b \lesssim 2\,\mathrm{Mpc}$, illustrating the challenges of accurately modeling and resolving galaxy formation physics. It is noteworthy that these differences are observed as far out as $\sim 2\,\mathrm{Mpc}$, indicating that the 'sphere-of-influence' of galaxies could extend to approximately ~ 20 times the halo virial radius ($\sim 100\,\mathrm{kpc}$). Current observations are very precise on these scales and can thus strongly discriminate between different galaxy formation models. We demonstrate that the Lyman-α absorption profile is primarily sensitive to the underlying temperature-density relationship of diffuse gas around galaxies, and argue that it thus provides a fundamental test of galaxy formation models.

Модельные газовые окрестности модельных темных гало

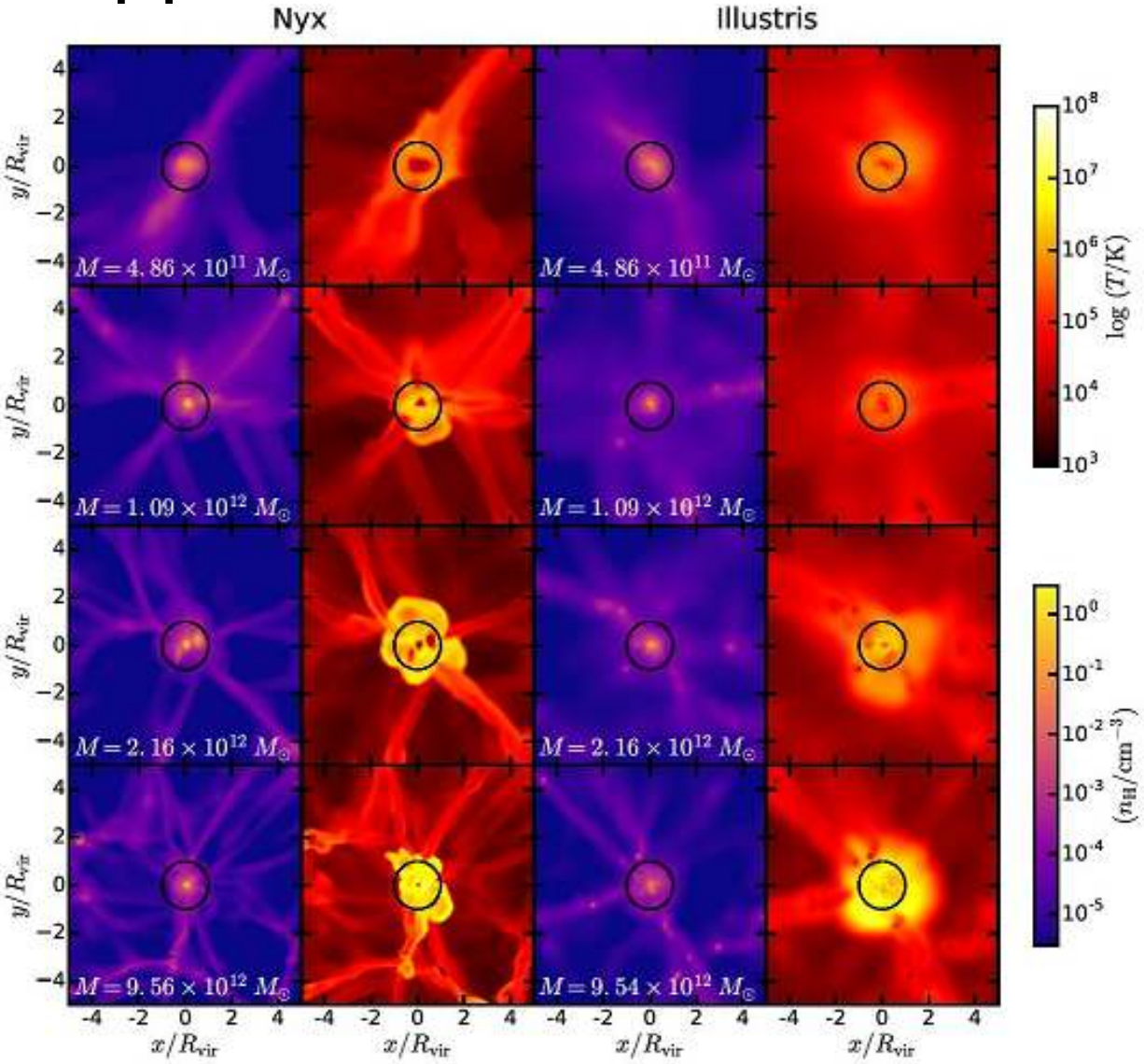

А это уже наблюдательная статистика в сравнении с моделями

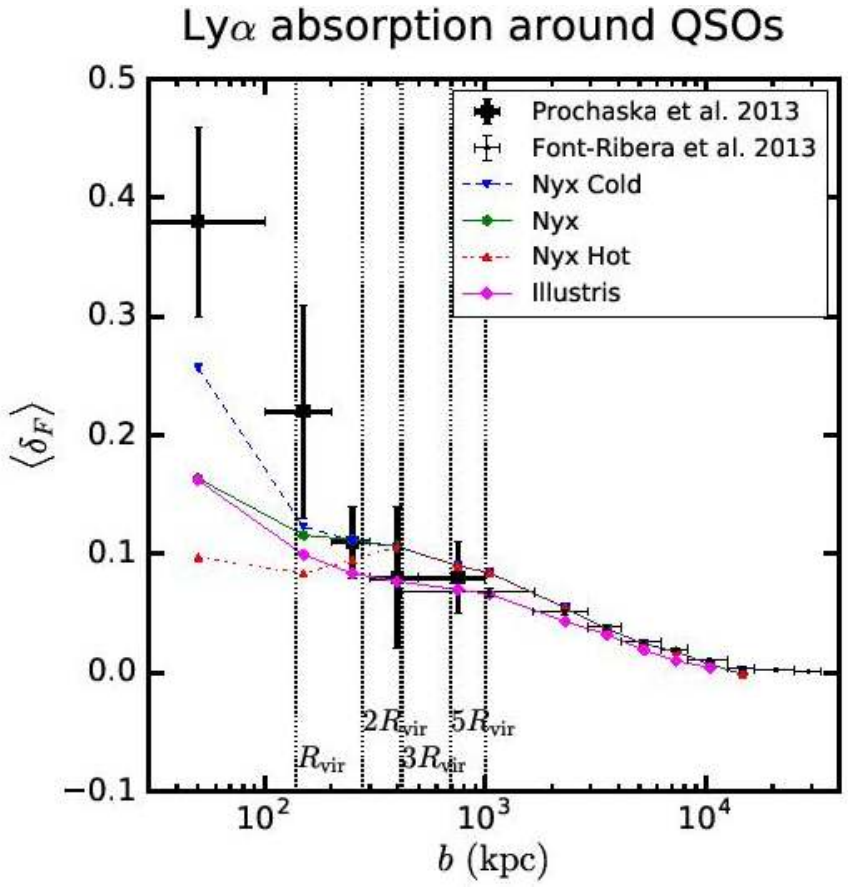

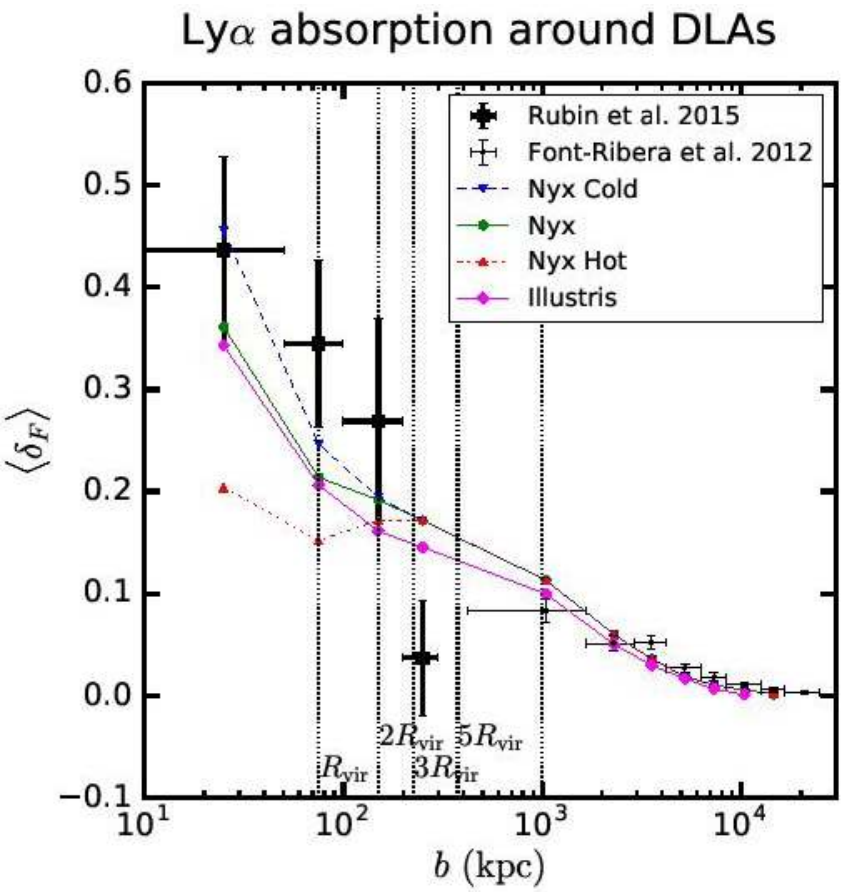

Модели недооценивают плотность HI внутри вириального радиуса

Astro-ph: 1709.04474

ILLUMINATING LOW-SURFACE-BRIGHTNESS GALAXIES WITH THE HYPER SUPRIME-CAM SURVEY

JOHNNY P. GRECO[1], JENNY E. GREENE[1], MICHAEL A. STRAUSS[1], LAUREN A. MACARTHUR[1] XZAVIER FLOWERS[1,9], ANDY D. GOULDING[1], SONG HUANG[2], JI HOON KIM[6], YUTAKA KOMIYAMA[3,4], ALEXIE LEAUTHAUD[2], LUKAS LEISMAN[8] ROBERT H. LUPTON[1], CRISTÓBAL SIFÓN[1], SHIANG-YU WANG[7]

[1] Department of Astrophysical Sciences, Princeton University, Princeton, NJ 08544, USA

[2] Department of Astronomy and Astrophysics, University of California, Santa Cruz, 1156 High Street, Santa Cruz, CA 95064 USA

[3] National Astronomical Observatory of Japan, 2-21-1 Osawa, Mitaka, Tokyo 181-8588, Japan

[4] Department of Astronomy, School of Science, Graduate University for Advanced Studies (SOKENDAI), 2-21-1, Osawa, Mitaka, Tokyo 181-8588, Japan

[5] Kavli Institute for the Physics and Mathematics of the Universe (Kavli IPMU, WPI), University of Tokyo, Chiba 277-8582, Japan

[6] Subaru Telescope, National Astronomical Observatory of Japan, 650 N Aohoku Pl, Hilo, HI 96720

[7] Institute of Astronomy and Astrophysics, Academia Sinica, P. O. Box 23-141, Taipei 106, Taiwan

[8] Department of Physics and Astronomy, Valparaiso University, Valparaiso, IN 46383, USA

[9] Florida Institute of Technology 150 W. University Blvd Melbourne, Florida 32901

ABSTRACT

We present our catalog of extended low-surface-brightness galaxies (LSBGs) identified in the Wide layer of the Hyper Suprime-Cam Subaru Strategic Program (HSC-SSP). Using the first $\sim$200 deg^2 of the survey, we have uncovered a rich diversity of LSB phenomena, including red ($g - i \geq 0.64$) and blue ($g - i < 0.64$) LSBGs with a wide range of morphologies, tidal debris from galaxy interactions, and cirrus emission from Galactic dust. We publish a catalog of 781 LSBGs, which, because we focus on angularly extended galaxies

Бимодальность по цвету?

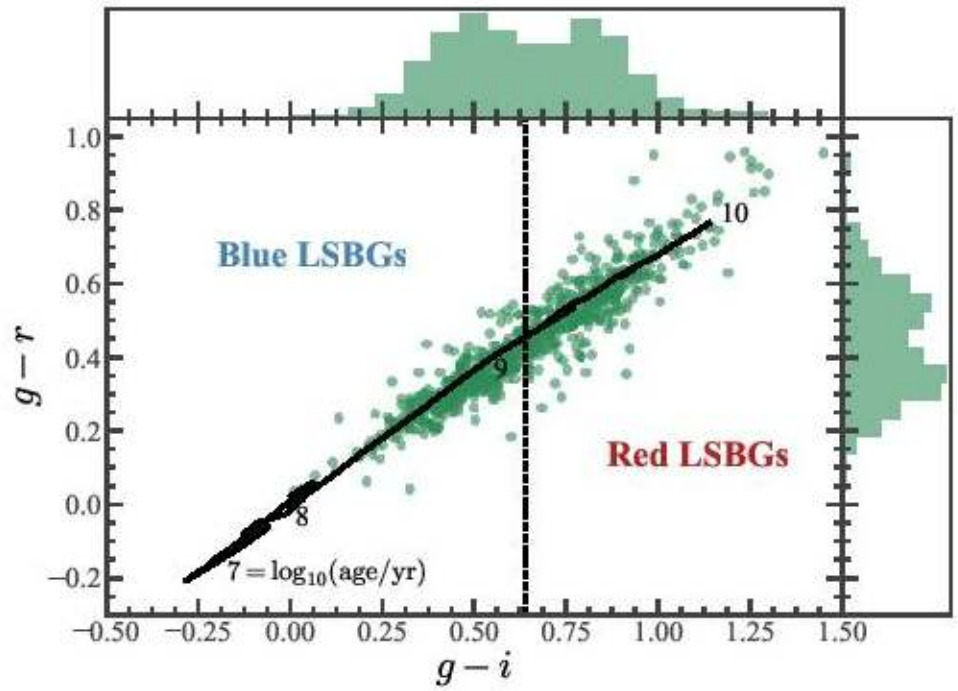

Figure 3. Color-color diagram for our full catalog of LSBGs. We separate the galaxies into red ($g-i \geq 0.64$) and blue ($g-i < 0.64$) subsamples, with the dividing color at the median value. We show the evolutionary path of a $0.4\times$solar metallicity simple stellar population from the models of Bruzual & Charlot (2003). The subsolar and solar metallicity models fall on very similar evolutionary paths in this color space. Note the apparent bimodality in both the $g-r$ and $g-i$ color distributions shown on the top and right side of the figure.

Распределение на небе

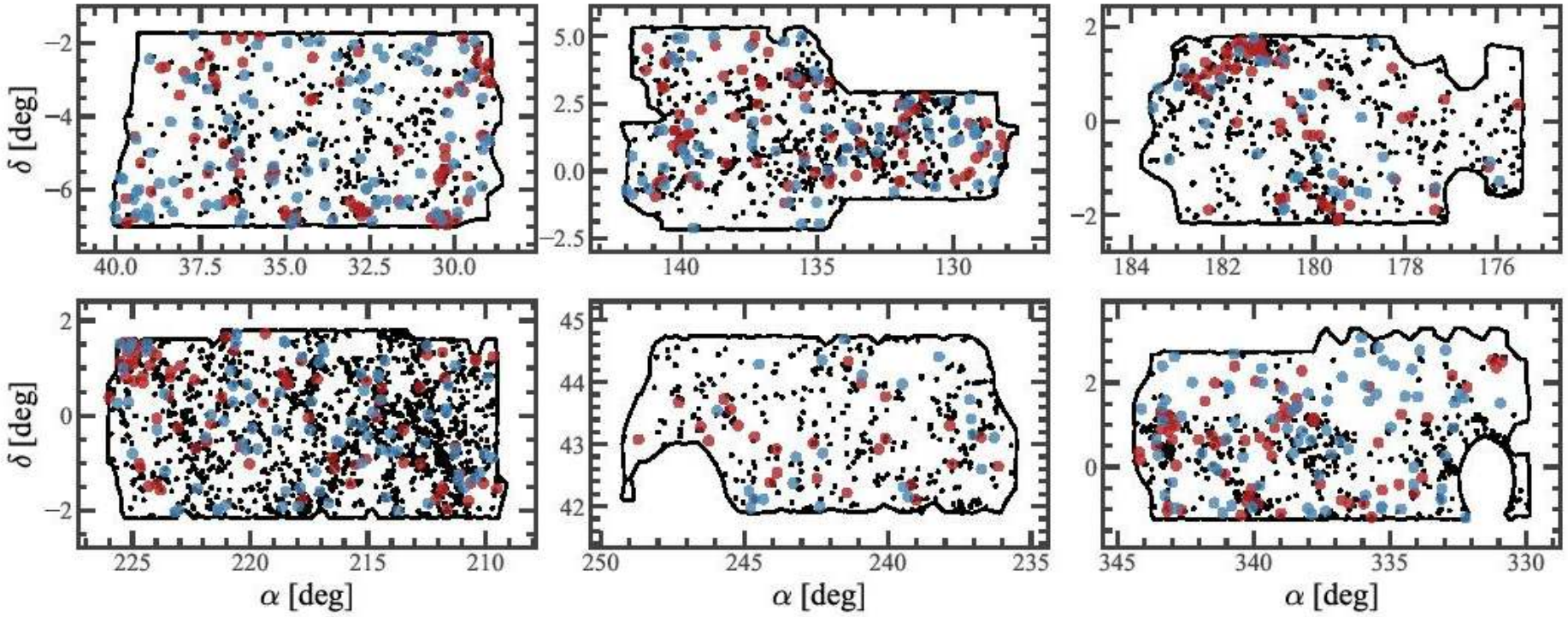

Figure 5. Sky positions of LSBGs within the HSC-SSP fields that have been observed to the full Wide layer depth (in gri) as of the internal S16A data release (see Aihara et al. 2017a for information about the HSC-SSP data releases). Red LSBGs ($g - i \geq 0.64$) are colored red, and blue LSBGs ($g - i < 0.64$) are colored blue. We also show the positions of galaxies with $z < 0.055$ (black points) from the NASA-Sloan Atlas (NSA) galaxy catalog.

Примеры LSB-галактик

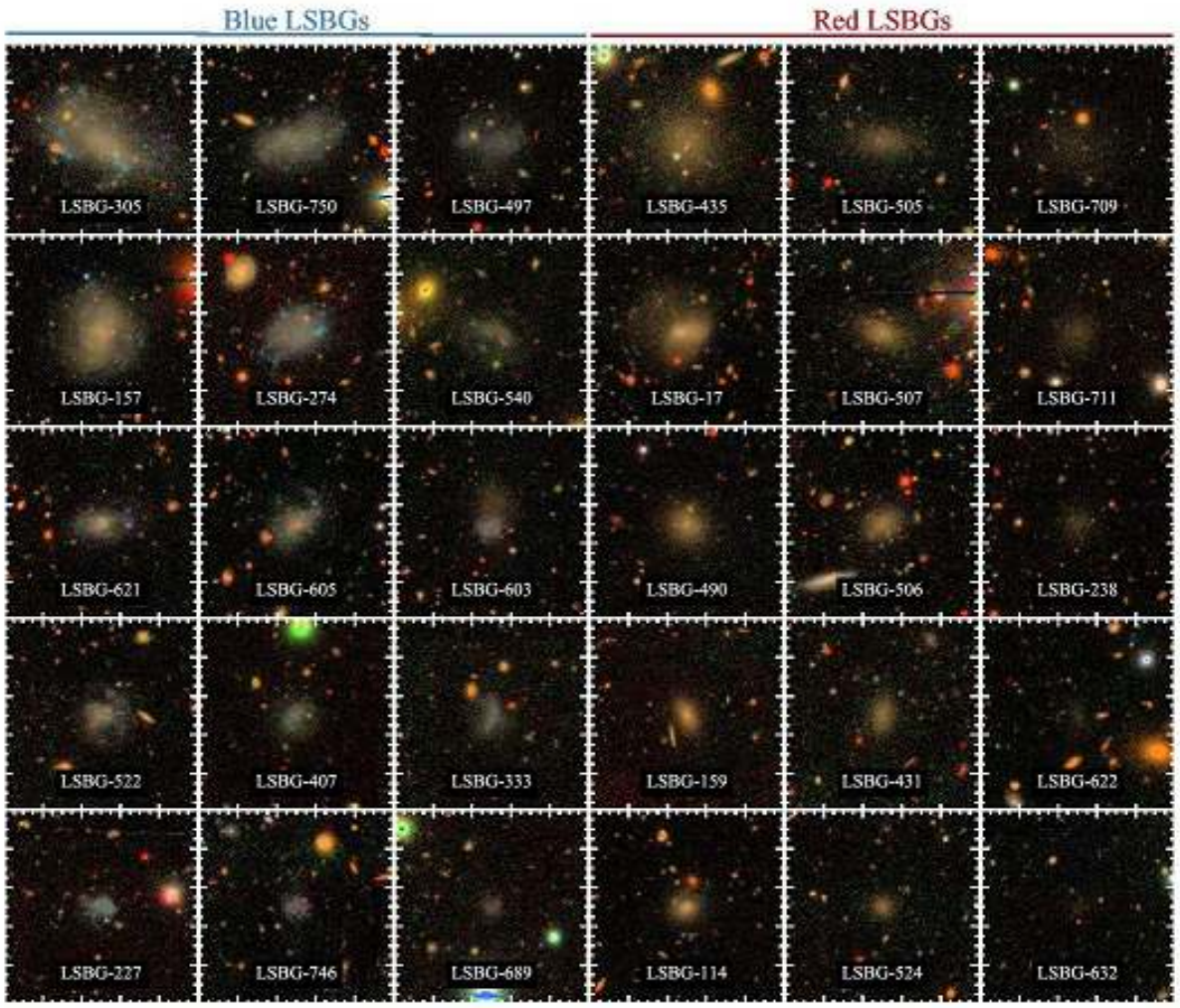

Figure 4. HSC-SSP gri-composite images (Lupton et al. 2004) of representative blue (left; $g - i < 0.64$) and red (right; $g - i \geq 0.64$) galaxies from our LSBG sample. Each cutout is 55″ on a side. For each subsample, size (surface brightness) roughly deceases from top to bottom (left to right). The blue galaxies are generally irregular, star-forming systems, whereas the red galaxies tend to be elliptical and quenched.

Экспоненциальные профили, у красных – диапазон пов. яркостей

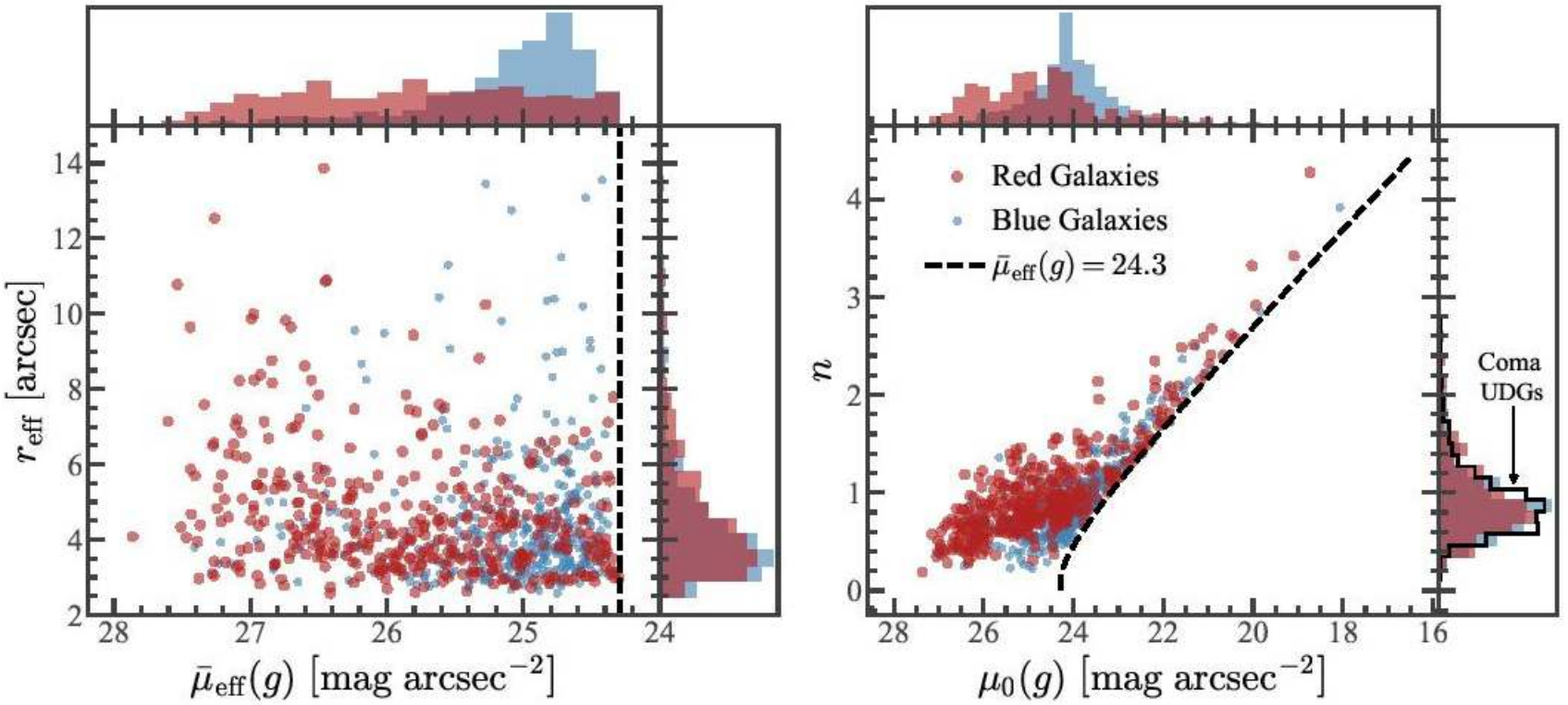

Пухлые диски?

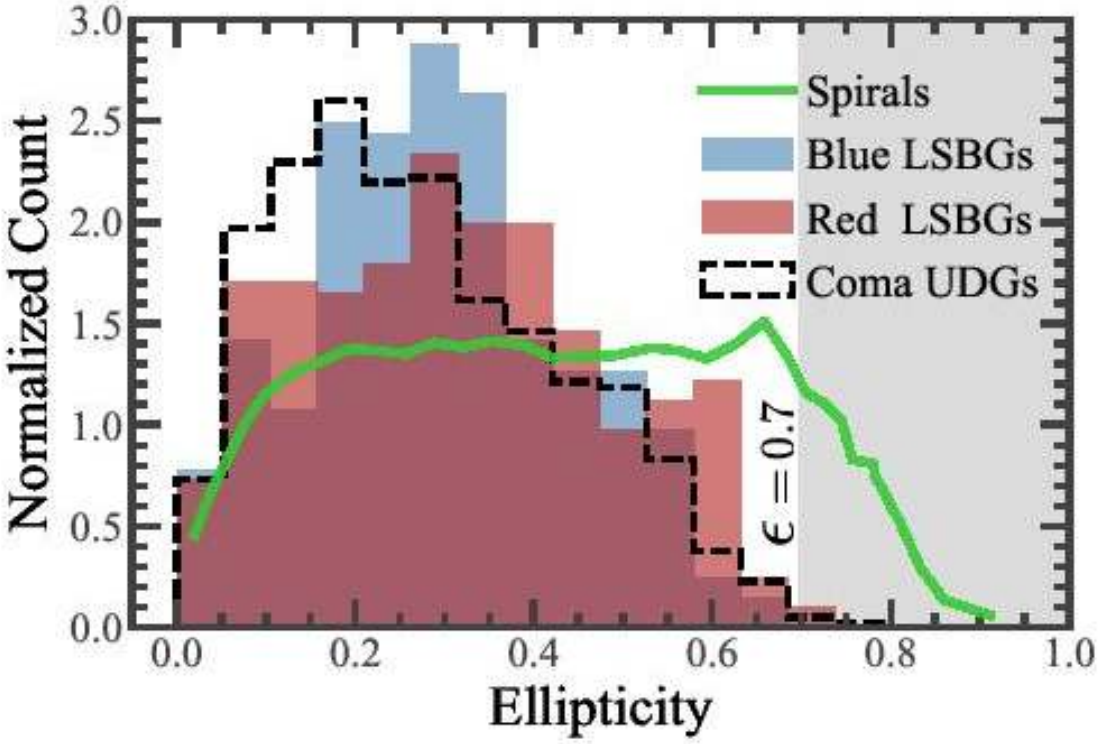

Figure 7. Ellipticity (ϵ) distributions of our red and blue LSBG subsamples, UDGs in the Coma cluster (Yagi et al. 2016), and spiral galaxies from SDSS (Rodríguez & Padilla 2013) that were classified by the Galaxy Zoo project (Lintott et al. 2008). We select galaxies with $\epsilon < 0.7$; values outside this range are shaded gray.

GALEX: Ультрафиолет у 50%, в том числе у некоторых красных

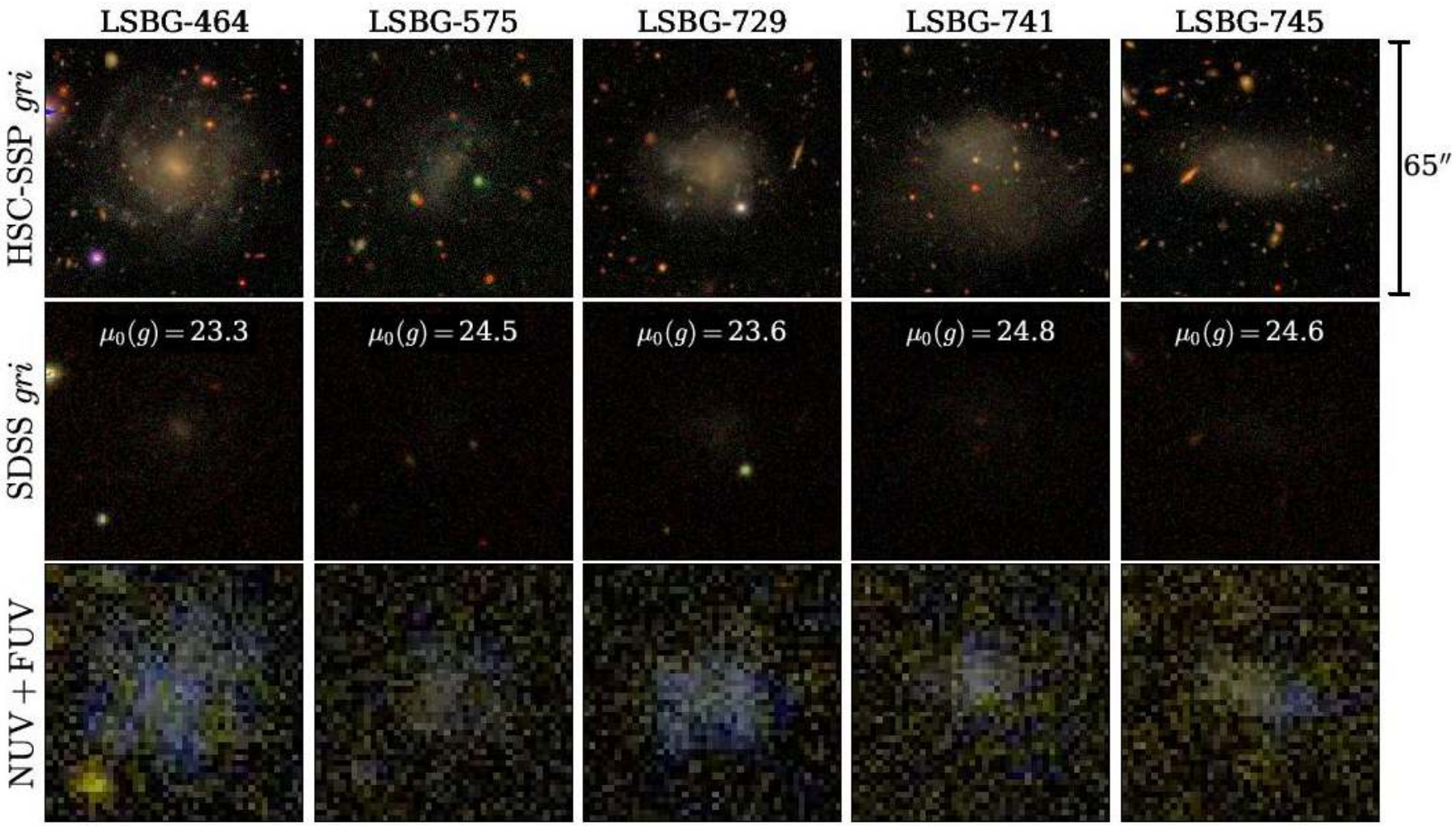

Разнообразные морфологии? Родственные связи?

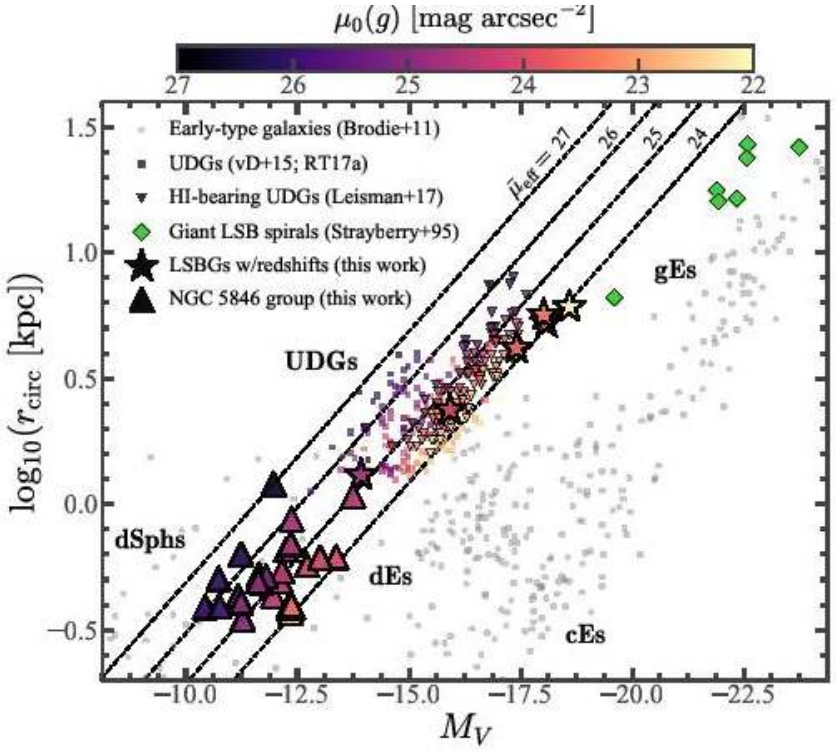

Figure 11. Size-luminosity relation for LSBGs in our sample for which we have distance information. Stars show LSBGs with archival spectroscopic redshifts, and large triangles show LSBGs that are projected in close proximity to the NGC 5846 group (see Figure 10), which is at a distance of 26.1 Mpc (we assume this distance for these LSBGs). We also show the family of early-type galaxies (Brodie et al. 2011), giant LSB spiral galaxies (Sprayberry et al. 1995), UDGs from van Dokkum et al. 2015 (vD+15) and Román & Trujillo 2017a (RT167a), and H I-bearing UDGs (Leisman et al. 2017). The color bar shows the g-band central surface brightness for LSBGs